Current Approaches and Challenges in Advanced Oxidation Processes for Nanoplastic Degradation

Arezou Fazli*, Athanassia Athanassiou, Despina Fragouli*

[a] *Smart Materials, Istituto Italiano di Tecnologia, via Morego 30, 16163 Genova, Italy*

* Corresponding authors:

Arezou.fazli@iit.it (A. Fazli)

Despina.Fragouli@iit.it (D. Fragouli)

Keywords

Nanoplastic remediation; Nanoplastic pollution; Environmental fate of nanoplastics; Nanoplastic characterization; Advanced oxidation process.

Abstract

The proliferation of plastic production has led to a surge in nanoplastics (NPs) pollution, posing significant environmental and health risks. Despite efforts to mitigate plastic waste, NPs persist as a significant challenge due to their small size, high surface-to-volume ratio, and complex nature. This review explores advanced oxidation processes (AOPs) as promising techniques for NP remediation, including ozonation, electrochemical, photocatalytic, and plasma-induced processes. Existing research is analyzed to investigate the performance of AOPs in NP degradation. Gaps in the development of effective processes and analytical methods are highlighted, and future directions are suggested. This review aims to enhance understanding and promote sustainable solutions for the remediation of NPs from contaminated water resources in alignment with the objectives outlined in the sixth Sustainable Development Goal set by the United Nations.

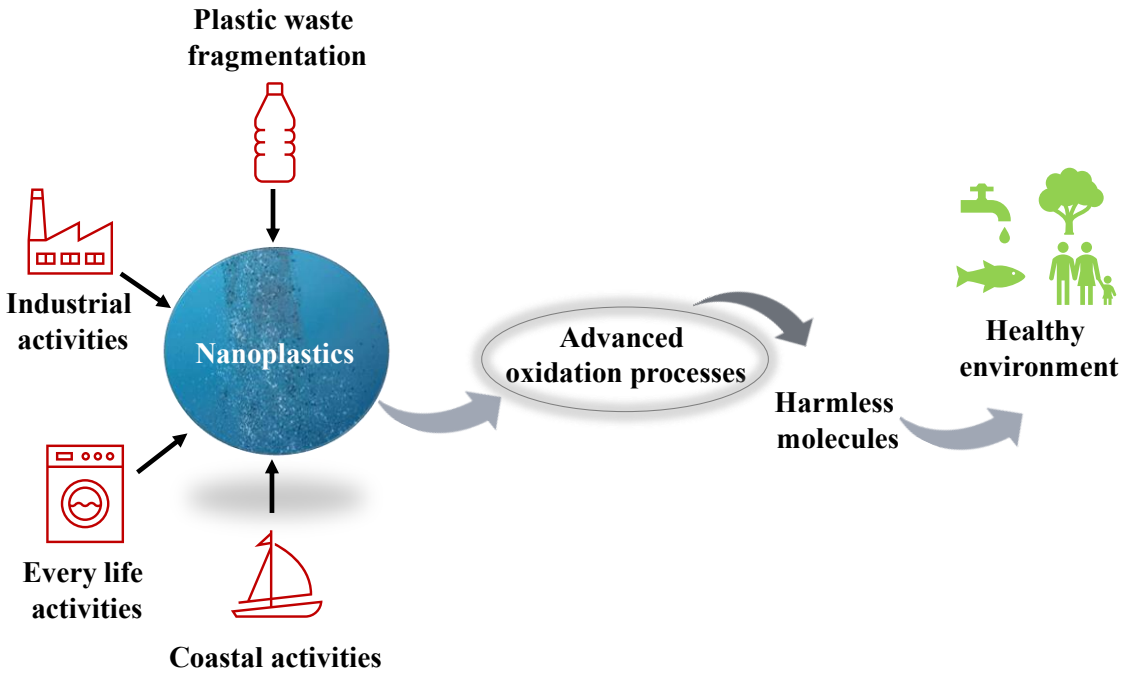

A list of acronyms and abbreviations

AOPs

Advanced oxidation processes

AFM

Atomic force microscopy

DF-HIS

Dark-field hyperspectral microscopy

DLS

Dynamic light scattering

DSC

Differential scanning calorimetry

EDX

Energy-dispersive X-ray spectroscopy

ELS

Electrophoretic light scattering

FESEM

Field emission scanning electron microscope

FETEM

Field emission transition electron microscope

FFF

Field-flow fractionation

FTIR

Fourier transform infrared spectroscopy

GPC

Gel permeation chromatography

HPLC

High-resolution liquid chromatography

ICP-MS

Inductively coupled plasma mass spectrometry

MPs

Microplastics

NMR

Nuclear Magnetic Resonance

NPs

Nanoplastics

NOMON

Nanoro-M model optical nanoscope

NTA

Nanoparticle Tracking Analysis

O_3

Ozone

PET

Polyethylene terephthalate

PS

Polystyrene

Pyr-GC/MS

Pyrolysis gas chromatography-mass spectrometry

SEM

Scanning electron microscopy

SERS

Surface-enhance Raman spectroscopy

TD-PTR-MS

Thermal desorption-proton-transfer reaction

TEM

Transition electron microscope

TOC

Total organic carbon

XAFS

X-ray absorption fine spectra

XPS

X-ray photoelectron spectroscopy

1. Introduction

The introduction of the concept of polymerization by Herman Staudinger in 1920 led to a better understanding of polymer chemistry and, therefore, to the more massive production of plastic worldwide [1]. Plastic has multifaceted properties, such as low thermal conductivity, lightweight, ease of preparation, ability to take different forms and shapes, and tunable mechanical properties [2]. For these reasons, plastic is an essential component of various materials in applications such as agriculture, textiles, medical and electronic devices, personal care products, vehicles, packaging, toys, etc. [3]. The high demand for plastic materials is reflected by global plastics production, which has significantly increased over the past 60 years, from 15 million tons in 1964 to 400.3 million tons in 2022, and continuing at this pace, it is expected to duplicate over the next 20 years [4–6]. On top of this, recent research studies indicate that the recent COVID-19 pandemic increased even more plastic needs [7].

Although the plastic production continues to increase, the recycling rate remains low. Studies have shown that only 9 % of the yearly produced plastic waste is recycled, with the rest ending up in the environment through various pathways [8,9]. Even though multiple efforts have been made so far to pose some management policies for the limitation of plastic waste through the control of plastic production, utilization and end of life, the use of biodegradable plastics, and the improvement of the recycling processes [3], there is still a considerable amount of plastic waste present in the environment.

Oceans and rivers are estimated to receive nearly 13 million tons of plastic waste annually [10]. Plastic debris in water bodies is present in the form of macroplastics (>1cm), mesoplastics (1–10 mm), microplastics (MPs, 1-1000 µm), and nanoplastics (NPs). Plastic particles with sizes below 1 µm are generally considered as NPs; however, for the sake of conformity with the definitions of

nanomaterials, Hartmann et al. [11] recently proposed the subdivision to submicron-plastics with sizes ranging between 100 nm and 1 μm and NPs with sizes below 100 nm. Nonetheless, the present review considers NPs as plastic particles with sizes smaller than 1 μm.

Recent research suggests that MPs and NPs exacerbate environmental pollution due to their destructive effects on aquatic organisms and human health. It has been proved that MPs and NPs can affect the growth rate of marine organisms and enhance their mortality rate [2], while on a cellular scale, they can cause gene expression variations and a high cell death rate [12,13]. NPs and MPs may accumulate in the organs and cause some disorders in living bodies. In contrast, NPs can quickly enter the bloodstream due to their small size, permeate cellular barriers or cell membranes, and alter their functionalities [12].

For the above reasons, NPs are emerging water pollutants of significant concern even in low environmental concentrations. Their characteristics make it challenging to perform on-site detection and monitoring, study their environmental and biological fate, and evaluate processes for their remediation. Various advanced characterization methods have been developed to contrast the difficulties of detecting and analyzing such organic particles [14],demonstrating their capability to efficiently track small amounts of NPs in impure samples [14,15]. Although significant steps forward have been made, current studies on the NPs' fate are mainly conducted using artificial NPs and controlled environments, with the risk of missing some critical parameters for the transition from the laboratory to the environmental conditions.

Due to their small size, non-biodegradable nature, and presence in complex water bodies, NPs are very difficult to be removed from the water environment. Nonetheless, water treatment technologies that have demonstrated the ability to remove NPs of well-known chemistry from controlled, artificial environments have been recently reported, such as adsorption/aggregation

[16,17], coagulation [18], flocculation [19,20], sedimentation [21], biological [22] and membrane filtration [23]. Nonetheless, most of these methods can remove NPs only partially from water samples. At the same time, some of the remediation processes, such as coagulation/flocculation, require the presence of additional chemicals in the systems, which may produce secondary pollution. To address these problems, advanced oxidation processes (AOPs) have been recently reported to be among the most promising methods for the remediation of NPs, as they can provoke the mineralization of MPs and NPs while producing limited secondary pollution [24].

AOPs, such as electrochemical [25], ozonation [26], and photocatalytic [27–30] processes, are newly emerged methods in the field of NPs degradation. However, the small size of the NPs and their complex organic nature limit their characterization and analysis during the treatment process. Therefore, diagnosing potential problems to achieve highly efficient degradation of NPs using AOPs remains a challenge. To do so, data collected from the recently published studies should be reported, compared, and commented on. However, to the best of our knowledge, the current literature lacks a review article that assesses the effectiveness of AOPs in degrading nano-sized (<1 μm) plastic particles and explores recently applied characterization methods.

Hence, herein, we review the available research studies focused on AOPs for the degradation of NPs in water. We offer a critical discussion on their feasibility and effectiveness and a general perspective for future works. In this context, we first focus on I) the sources of NPs and their hazards as water contaminants, II) the use of different remediation strategies for the degradation of NPs, III) the applied AOPs on the in situ degradation of NPs, and IV) the current research gaps and perspectives in degrading NPs through AOPs. With this review paper, we aim to highlight and optimize the potentiality of sustainable AOP methods in the degradation of NPs and to give an

overall view of the effective characterization and analysis methods to promote accuracy in this field.

2. Principal sources and hazards of NPs

MPs and NPs are classified as primary or secondary depending on their sources. Primary plastic particles are components of market products, and they enter the environment directly through these products. Industrial abrasives, cosmetics and exfoliating personal care products, adhesives, electronics, paints, and drug delivery medical devices are well-known examples of commercially available products that contain primary MPs and NPs [12,13,31]. Alternatively, all the discarded plastic products, such as plastic bags, bottles, ropes, fishing nets, food packaging, and electronics, can be sources of secondary MPs and NPs [31,32]. These particles derive from the breakdown of plastic debris caused by physical, chemical, and biological actions such as hydrolysis, photodegradation, mechanical abrasion, and biodegradation [32,33]. For instance, Lambort et al. [34] proved that polystyrene (PS) coffee cups could be degraded to MPs and subsequently to NPs under UV and visible light irradiation. In addition, Prenner et al. [35] demonstrated that rubber tires can produce NPs during constant friction in particular driving conditions (high speed and sharp brake) [36]. Accordingly, a study has shown that in 2018 in Austria, about 6% of the used rubber tires were emitted into the air as micro- and nano-sized particles [35]. Moreover, Dawson et al. [37] reported that the Antarctic krill can transform MPs into NPs through digestive fragmentation, proving that NPs can be generated by ingesting MPs in marine species.

Regarding environmental pollution, the distribution of NPs in water has become an emerging environmental issue. Fig. 1 provides an overview of the significant sources of NPs in water. Water bodies are polluted by macroplastics and MPs wastes, which are produced directly through sea-

based activities (e.g., fishing gears) but also land-based activities, such as inadequate waste disposal and management, industrial activities, municipal sewage and sludge, tire abrasion, and surface waters runoff, and eventually pass to the oceans through different pathways like wind, water, and soil [38,39] Chemical, physical, and biological transformation of such plastic litter in water results in NPs [33,37]. In addition, although wastewater treatment plants (WWTPs) limit the dispersion of water pollutants, they can be a significant source of MPs and NPs. Concerning MPs, it is estimated that 25% of the globally released MPs in the environment are attributed to the WWTPs [10]. In the case of NPs, although there is no precise information about the amount, such small particles can undoubtedly pass through the various water treatment stages and be released together with the MPs in the environment or can even be generated from the fragmentation of the MPs, through shear stress forces during the treatment processes [10].

A recent study on the biological fate of NPs of two different sizes (i.e., 50 and 500 nm) showed that the nonfunctionalized PS NPs of larger size (500 nm) can be accumulated in the digestive organs of aquatic animals. In contrast, smaller NPs (50 nm) can penetrate tissues, cause immune system disorders, and increase marine organisms' growth rate [40]. In addition, the functional groups and the high surface area of NPs allow the adsorption and transport of various water pollutants such as heavy metals or endocrine disruptors (i.e., perfluorooctane sulfonate, bisphenol A), as well as the effective release of various endogenous pollutants originating from the components used in the production of plastic [41].

Concerning human exposure, as depicted in Fig. 1, NPs may enter the human organs through ingestion, inhalation, and dermal adsorption [42]. Dermal adsorption of NPs can occur using personal skin care products containing such NPs. On the other hand, ingestion of plastic NPs is likely the main pathway of entry into human organs since they can be ingested by consuming

contaminated food, like seafood, salt, and beer, or by drinking contaminated water [42,43]. Their small size, high surface area, and surface charge will likely raise diverse adverse effects. Recent experimental findings suggest that NPs can contribute to the development of neurodegenerative diseases. In-vivo studies on mice proved that the oral ingestion of NPs (30–50 nm) may reach the brain tissue and induce cognitive dysfunction [44]. Moreover, in vitro studies proved that NPs (30 nm) can penetrate human neural stem cells through endocytosis, where they accumulate, leading to decreased cell proliferation and eventually death [45]. Marfella [46] carried out an in-depth observational study on the correlation between the presence of MPs and NPs in the carotid artery and a higher risk of heart attack, stroke, or death. To do so, they focused on patients undergoing surgery for carotid artery disease. Upon analysis, it was found that out of 257 patients, 150 had polyethylene particles in their carotid artery plaques (21.7 ± 24.5 μg/mg of plaque), while 31 patients had polyvinyl chloride (5.2 ± 2.4 μg/mg of plaque).

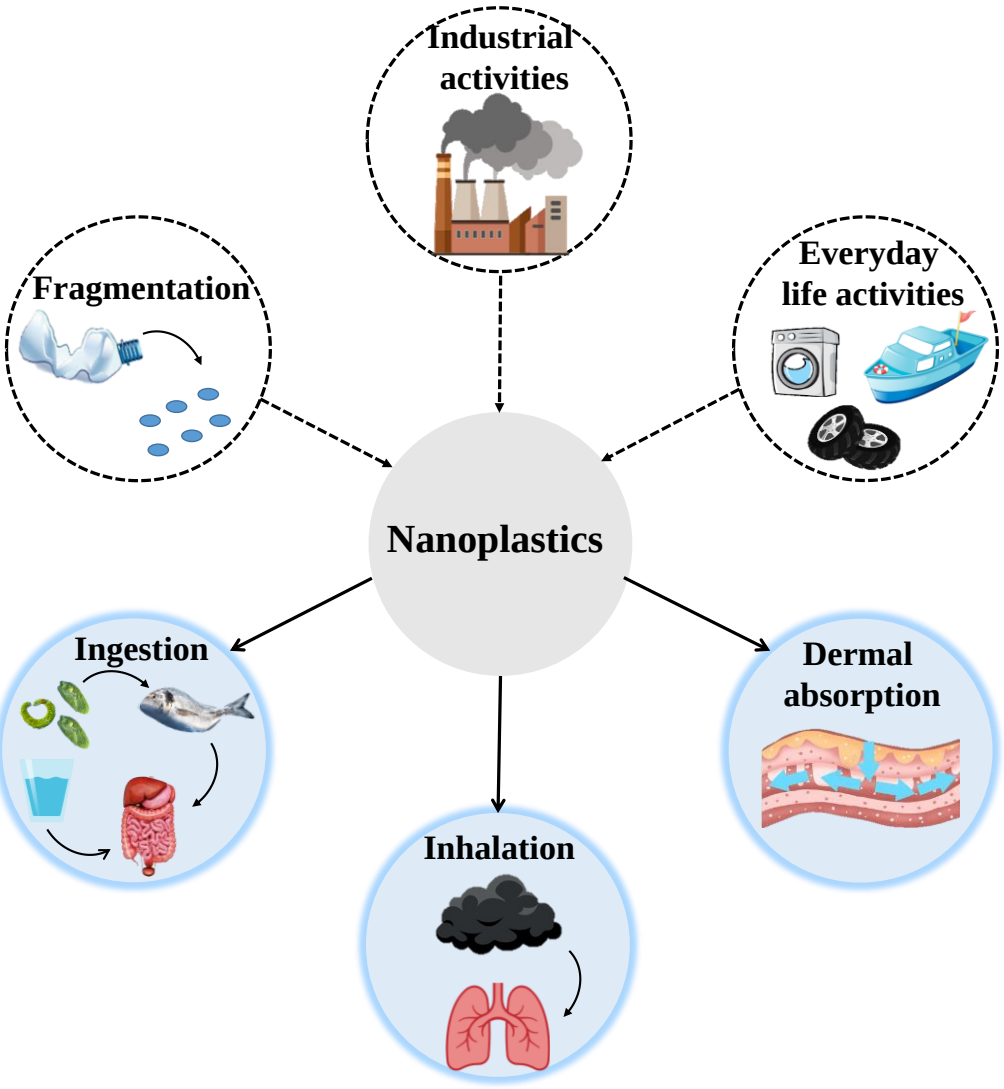

Fig. 1. A general summary of sources producing NPs in water and pathways to human exposure.

3. Remediation strategies for NPs contamination in water

There is increasing evidence that drinking water is contaminated with plastic particles, making it a significant source of human exposure [47]. Kosuth et al. [48] studied the presence of MPs in tap and bottled water. Samples from 14 countries were subjected to vacuum filtration (cut-off: 2.5 μm), and the filters were visually assessed using a dissecting microscope. The results showed that 81% and 93% of the tap and bottled water samples, respectively, were contaminated with MPs,

mostly with fibers of length ranging from 0.1 to 5.0 mm. Moreover, Li et al. [47] have recently shown the existence of NPs in tap water. The collected samples, subjected to successive filtration steps, revealed the presence of NPs with concentrations ranging between 1.67 and 2.08 μg L^{-1}, depending on their size (from 255 nm to 58 nm), with most of them composed of PS, polyvinyl chloride, polyolefins, and polyamide. Furthermore, Huang et al. [49] analyzed polyethylene terephthalate (PET) bottled water using a tangential flow ultrafiltration system. The final retentate fluid was examined through a new nanorod-M super-resolution optical microscopy system equipped with a super-resolution microsphere amplifying lens. Their results revealed the presence of organic particles in the water with sizes in the micron, submicron, and nanosized range. In brief, NPs can be found in potable water, either surviving different water treatment processes or being released from the plastic bottles where they are stored. Therefore, there is an essential need to control and eliminate their presence through efficient water treatment processes. This section reviews some recently published papers on removing NPs following standard water treatment methods like coagulation, flocculation, sedimentation, filtration, adsorption, and bioremediation.

Since coagulation or flocculation methods are the typical first steps in water purification, they have also been considered for removing NPs from contaminated water. Chen et al. [20] declared the high potential of Mg and Al-based layered double hydroxides (Mg/Al-LDHs) for the flocculation of PS NPs with sizes ranging between 0.05 and 0.10 μm. In particular, it has been demonstrated that at specific pH values, during the flocculation process Mg/Al-LDHs can be formed in situ, and simultaneously, during their formation can capture existing PS NPs in their layers. Such Mg/Al flocculants can remove about 90.0% of the PS NPs by the liquid media. However, a significant challenge for the practical application of this method is the need to separate the LDH-encapsulated NPs from the treated water. Alternatively, Zhang et al. [18] studied the removal of fluorescent PS

NPs (180 nm) from drinking water through coagulation-flocculation combined with sedimentation (CFS). As reported, even with the coagulant help, the NPs were not removed upon the application of CFS. Their results point toward a general rule that such water treatment processes are inefficient for removing hydrophobic NPs that effortlessly float on water due to their low density. Nonetheless, the same study proved the high ability of column filtration to remove NPs (180 nm) with an efficiency of 99% as due to their small size, they are likely to attach to (or to be absorbed to) the grains. Although this method seems to work well, some NPs still pass through the filter and can be found in water, while the removal efficiency is reported to depend on the particles' size (180 nm–125 μm). On top of this, the used NPs were composed of pure polymer and had a homogenous spherical shape. In environmental conditions, the NPs may arrive to much smaller sizes, while they are most likely characterized by shape inhomogeneity and altered surface chemistry. As previously referred, plastic fragments in water are exposed to different degradation processes and interactions with various components found in the environment, resulting in increased hydrophilicity or the formation of complexes. For instance, unlike pristine NPs, those in the environment undergo natural aging processes like UV irradiation or biological degradation. These processes change surface chemistry, introducing oxygen-containing functional groups [50]. Furthermore, in the case of environmental samples, NPs, and other organic and inorganic components may clog the filters and decline their efficiency for continuous water treatment [51].

Alternatively, various batch adsorption studies were conducted to demonstrate the efficiency of removing NPs from water. Ganie et al. [52] prepared sugarcane bagasse-derived biochar powders (BC) at different pyrolysis temperatures to assess their efficiency in adsorbing hydrophilic PS-based Latex beads (size: few hundreds of nm < 500 nm). The biochar prepared at the highest pyrolysis temperature (750 $^{\circ}$C) had a high surface area (540.36 $m^2 g^{-1}$) and enhanced pores volume.

At the same time, the performed analysis confirmed that it possessed the least negatively charged functional groups, all characteristics that improve the electrostatic interaction with the negatively charged NPs and their entrapment into the porous structure, reaching a maximum adsorption capacity of 44.9 mg/g in DI water dispersions. In another work, Tiwari et al. [53] studied the efficiency of Zn/Al LDH to adsorb hydrophilic PS NPs (55 nm). They reported that the zeta potential of LDH (45.5 ± 0.6 mV) became negative after the interaction with NPs (-36.8 ± 2 mV). At the same time, new absorption bands in the FTIR spectra appeared, and the surface area of the LDHs was enhanced, all supporting these structures' successful adsorption of NPs. Under optimized conditions, the maximum adsorption capacity reached was 164.49 mg/g in DI water.

Table 1 shows the most relevant studies on removing NPs of sizes lower than 500 nm through adsorption processes. Although the results are promising, some restrictions still make this method challenging. For instance, in all the recent studies, the adsorbents were in the form of particles dispersed in the reaction media, making their recovery after the remediation process, as centrifuge, filtration, or other separation steps should be applied for their removal. Moreover, only a few works have studied the fate of the adsorbed NPs after collecting the adsorbents, following chemical desorption steps, and studying the reusability. The complexity of the media where the NPs are found is still an issue. Although some of the studies have analyzed how the adsorption performance is affected by the presence of different components in the water medium, further studies in more complicated environments need to be performed. In addition, in most of the presented studies, the target NPs are made of pure PS of various sizes and with specific surface chemistry. However, it remains to be seen whether NPs of different nature and with different surface functional groups can show the same behavior under similar conditions.

Biological degradation is another attractive method for the remediation of plastic particles. Focused on NPs, Vogel et al. [22] studied the enzymatic hydrolysis of PET NPs mimicking real-world aquatic conditions through the thermophilic cutinase TfCut2 from *Thermobifida fusca*, demonstrating the effective cleavage of the polymer's ester bonds. However, the enzymatic and microbial degradation of NPs depends on the plastics' physico-chemical characteristics and on the required genes of the microorganisms to break them down [54]. Consequently, it is necessary to study the efficiency of biodegradation. Specific studies are needed for different types of NPs in complex environments to evaluate the performance of enzymatic biodegradation better.

Table. 1. Applied adsorbents for removing NPs from contaminated water.

Adsorbent	Adsorbent concentration (g L^{-1})	Type of NPs*	Particle size (nm)	NPs concentration mg L^{-1}	Removal capacity (mg g^{-1})	[Ref]
CuNi@C	0.3	PS	100	10	41.93	[55]
Fly ash modified with Fe ions.	0.02	PS	80	20	88.5	[56]
Mesoporous biochar	0.4	PS	100	20	56.02	[57]
Sugarcane bagasse-derived biochar (750 °C)	1.5	PS	<500	10	44.9	[52]
Zn/Al LDH	5	PS	55	250	164.49	[53]

***** In all studies, researchers used commercially available polystyrene NPs.

The above mentioned methods for plastic particle removal from water are often time-consuming, complex to implement, and necessitate significant space and large amounts of chemicals. Consequently, these factors limit their applicability [25,58]. Additionally, these methods cannot thoroughly eliminate severe and complicated water contaminants, such as plastic debris, allowing them to discharge into the environment from wastewater treatment plants quickly.

3.1. Advanced oxidation processes

AOPs have emerged as alternative methods for effectively remediating plastic particles in aqueous environment [59]. AOPs result in the in-situ generation of hydroxyl radicals (•OH), which undergo non-selective reactions and can degrade various organic pollutants with high-rate constants. Depending on the type of AOPs, other reactive oxygen species can also be generated, such as $O_2^{\bullet-}$, $SO_4^{\bullet-}$, $^1O_2$, $Cl^{\bullet}$, and $HO_2^{\bullet}$, which can contribute to the degradation of toxic compounds into harmless by-products [59,60].

Fig. 2 reveals that assessing the efficiency of AOPs for the degradation of plastic particles is in a preliminary stage, with most works targeting the degradation of MPs [61–64], while research on NPs is still minimal but increases progressively [26,27,65–67]. According to our search, one review paper assesses the effect of AOPs on the degradation of MPs [59]. In contrast, the published papers on the degradation of NPs were not considered in that review. Due to the small size of NPs, the challenges in conceiving their degradation mechanism and fate after AOPs and finding the most suitable characterization methods of the degradation products will need to be faced in future research works. In this section, we present the published outcomes, including experimental conditions and applied characterization methods, to give insights for future research on using the most promising AOPs in the degradation of NPs.

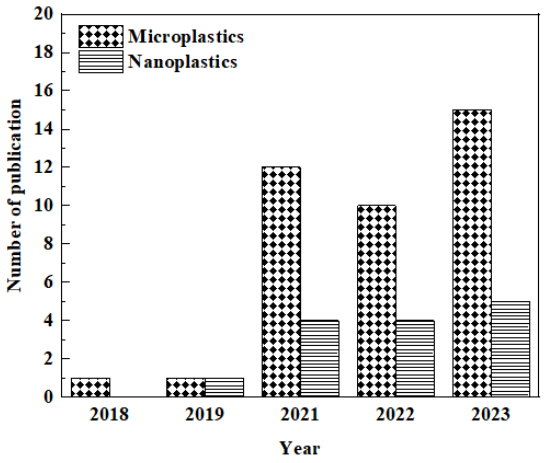

Fig. 2. The number of publications on using AOPs for the degradation of MPs and NPs per year. Literature search on Google Scholar with relevant keywords such as "advanced oxidation processes", "degradation of microplastics", and "degradation of nanoplastics".

The AOPs and the applied characterization methods to evaluate the NPs degradation are listed in Table 2. As shown, ozonation, electro-oxidation, phototransformation, plasma-induced degradation, homogenous/heterogeneous photocatalysis, and photoelectro-Fenton degradation are the AOPs that so far have been applied for the degradation of NPs in water. Detailed discussion regarding the effectiveness of these methods in the remediation of NPs in water will be provided in the subsequent sections.

Table 2. Experimental conditions, analytical methods, and efficiency of different AOPs in degradation of NPs (<1µm). (Please note that in the table, PS and PET refer to polystyrene and polyethylene terephthalate, respectively).

AOPs	Experimental conditions	Removal efficiency (%)	Applied analyses after the treatment and their outcomes	[Ref]
Ozonation	• NP Type: Commercial PS (100 nm) • [NPs]: 2.5 µg L^{-1} • [O_3]: 4.1 mg L^{-1} • pH: 6.43 • Reaction time: 240 min • Tested in distilled water	Mineralization†: 42.7%	• SEM: The surface of the NPs became rougher and their size smaller. • FTIR: = CH, - CH_2, -C=C- bonds were decreased and new peaks ascribed to C=O, -COC-, -CO- appeared. • XPS: The π- π* of the aromatic ring disappears, and the C=O peak appears. • Pyr-GC/MS: Phenyl rings were opened, producing aldehydes and ketones. • GPC: Molecular weight decreased during the process.	[26]

Ozonation	• NP Type: Synthesized Pd-labeled PS (> 100 nm) • [NPs]: 1.7 mg L^{-1} • [O_3]: 5 mg L^{-1} • pH: 7.90 • Reaction time: 45 min • Tested in lake water	No degradation was observed.	• SEM: No change in morphology and size of NPs was reported. • ICP-MS: Almost no Pd was detected in the treated water, implying no effect of ozonation in the destruction of NPs to release the trace element to the aqueous solution. • DLS: The hydrodynamic diameter of NPs was not changed.	[68]
Electro-oxidation	• NP Type: Commercial PS (100 nm) • [NPs]: 10 mg L^{-1} • [Na_2SO_4]: 0.007 M • pH: 5.00 • Reaction time: 380 min • Current density: 36 mA cm^{-1} • Anode: Boron-doped diamond • Cathode: Titanium and carbon felt	• With titanium cathode: Mineralization: 56.2% Degradation: 80.4% • With carbon felt: Mineralization: 63.8% Degradation: 92.8%	• UV/vis spectroscopy: the peak related to the absorption of C=C declined.	[25]
Plasma induced degradation	• NP Type: Commercial PS (200 nm) • [NPs]: 30 mg L^{-1} • Voltage = 19 kV	Information on degradation efficiency is not available.	• SEM: The NPs became rough, and some melted. • Nanoparticle potential analyzer: The particle size was reduced. Zeta potential became negative, illustrating the presence of –OH or –C=O groups on the NPs surface. • XPS: the appearance of O-containing groups. • FTIR: Carboxylated and hydroxylated compounds and -CH_3-containing molecules were reported. • UV/vis spectroscopy: The production of carboxylic acids was proved. • GC-MS: Short-chain carboxylated and hydroxylated by-products were generated. • Toxicity tests: The treated particles exhibited slightly more significant toxicity for *Scenedesmus obliquus* growth, while they were highly toxic for the *Human alveolar cells* A549.	[7]

Phototransformation	• NP Type: Synthesized ^{14}C-radioactively labeled PS (230 nm) • [NPs]: 100 m L^{-1} • Reaction time: 48 h • Light source: UV lamp (emission at 254 nm, 0.7 mW cm^{-2})	Mineralization: 17.1 %	• SEM: No change was observed. • FTIR: Carbonyl groups were formed. • Fluorescence spectroscopy: four main areas with fluorescence were observed, revealing the condensed aromatic rings with chains containing hydroxyl groups. • XPS: The oxygen content was increased, and the existence of C–O groups was proved. • HPLC-^{14}C-LSC: Oligomers and small molecules with relatively more carboxyl or hydroxyl groups demonstrated the chain scission.	[69]
Homogeneous photo-Fenton	• NP Type: Commercial PS (140 nm) • [NPs]: 20 mg L^{-1} • $[Fe^{3+}]_0$ = 1 mg L^{-1} • $[H_2O_2]_0$ = 130 g L^{-1} • pH_0 = 3 • Reaction time: 40 min • Light source: Medium pressure Hg lamp (150 W, 250 and 600 nm, 200 W m^{-2})	Mineralization: 100% Turbidity decrease: 100%	• Turbidity: A clear solution was obtained. • TEM: No particles were observed in the reaction media.	[70]
Homogeneous photocatalysis	• NP Type: Commercial PS (50-100 nm) • [NPs]: 5 mg L^{-1} • Reaction time: 360 min • Light source: low-pressure mercury UV lamp (6 W and 254 nm)	• With UV/NaClO: Turbidity decrease: 78.20% Mineralization: 7% • With UV/PMS: Turbidity decrease: 94.3% Mineralization: 63.90%	• SEM: The process did not affect the NPs shape. • Toxicity assessment: Inhibition rate of luminescent bacteria: 2.97%. • SEM: No spherical particles. • Toxicity assessment: Inhibition rate of luminescent bacteria: 98.19%.	[71]
Heterogeneous photocatalysis	• NP Type: Synthesized PS (318 nm) • [NPs]: 0.9% (w v^{-1}) § • Reaction time: 50 h • Semiconductor: TiO_2 • Immersed area: 1 cm^2 • UV lamp (0.021 mW cm^{-2})	Turbidity decrease:16.2 % • With TiO_2-barrier • With TiO_2-nanotubular:19.7 % With TiO_2- mixed: 23.5 %	• FTIR**:** Peaks attributed to carbonyl groups appeared. • GC-MS: The polymer chain has been decomposed, and carbonyl groups were formed.	[27]

	Heterogeneous photocatalysis	• NP Type: Polymethylmethacrylate (105 nm) • [NPs]: 300 mg L^{-1} • pH = 6.30 • Reaction time: 7 h • Semiconductor: TiO_2–P25/β- SiC foams • Light source: UVA lamp (15 W, emission at 354 nm, 112 W m^{-2})	Mineralization: 50 %	• Turbidity: Turbidity was decreased. • FTIR: CO, –OOH, and –OH groups appeared.	[29]
	Heterogeneous photocatalysis	• NP Type: Synthesized PS (350 nm) • [NPs]: 5 mg mL^{-1} • pH: 11.00 • Reaction time: 50 h • Semiconductor: Immobilized copper oxide • Immersed Area: 2.6 cm^2 • Light source: LED (50 W, emission at 400-800 nm, 5.3 mW cm^{-2})	Mineralization: 15% Degradation: 23.5%	• FTIR: Formation of C=C=O, C=C, and C=O corresponding to ketone, alkenes, and carbonyl groups. • GC-MS: Six intermediates were detected, revealing the breakdown of NPs.	[28]
Heterogeneous photocatalysis	**Batch slurry mode**	• NP Type: PS (140 nm and 300 nm) • [NPs]: 100 mg L^{-1} • Semiconductor: TiO_2-P25 • Light source: UV-A lamp (Philips 24 W/10/4 P lamps, 365 nm, 60 W m^2)	Information on degradation efficiency is not available.	• FE-SEM: NPs size reduction and shape modification. • DLS: Size reduction. Larger particles also appeared, suggesting aggregation. • FTIR: C=O and Peroxyl (C–O–O) groups emerged during the reaction. Carbonyl Index (CI) and Peroxyl Index (PI) increased over time, with a more pronounced evolution observed for CI.	[66]
	Immobilized mode	• NP Type: PS 140 nm and 508 nm • [NPs]: 20 mg L^{-1} • Semiconductor: TiO_2-P25 fixed on β-SiC foam • Light source: 4 UV-A lamps (Philips T5 15 W 10 Actinic BL, 365 nm, 110 W m^2)	• Using 140 nm NPs Mineralization: 80% • Using 508 nm NPs Mineralization: 68%	• pH reduction confirms the production of carboxylic acid-type by-products during the reaction. • FE-SEM and TEM: Modifications of the size and shape. • Py-GC/MS: The analysis revealed a good correlation between the direct TOC values and those derived indirectly from py-GC/MS analyses.	

Heterogeneous photocatalysis	• NP Type: Top-down chemical fabrication of PET NPs (111 ± 51 nm) from commercial bottles • [NPs]: 100 mg L^{-1} • pH = 3 • Reaction time: 5 h • Catalyst: 0.125 g/L immobilized TiO_2/MOF • Immersed Area: Held on a fine mesh stainless steel basket (4.2 ×4.2 ×4.4 cm) • Light source: Xenon lamp (Wavelengths consistent with sunlight, 30 W m^{-2})	Turbidity reduction: 54.6%	• FTIR: The carbonyl index was increased.	[72]
Heterogeneous photoelectro-Fenton	• NP Type: Commercial PS (215 nm) • [NPs]: 25 mg L^{-1} • [H_2O_2] = 0.5 mol L^{-1} • [Na_2SO_4] = 0.05 mol L^{-1} • pH = 2 • Flow rate: 50 µL min^{-1} • Catalyst: Immobilized MOF-derived porous Fe_2O_3 • Immersed Area: 2.5 cm^2 • Light source: Xenon lamp (Wavelengths consistent with sunlight, 120 mW cm^{-2}) • Bias voltage: 1.2 V	Degradation: 80%	• Fluorescence spectroscopy: Monitoring of the turbidity modification.	[65]
Heterogeneous piezo-photocatalysis	• NP Type: Commercial PS (100 nm) • [NPs]: 100 mg L^{-1} • pH = 7 • Reaction time: 15 h • Catalyst: 0.31 g/L SnO_2/g-C_3N_4 immobilized on poly (vinylidene fluoride-co-hexafluoropropylene) (3 ×3 cm^2) • Light source: Xenon lamp (Wavelengths consistent with sunlight, 100 mW cm^{-2})	Mineralization: 46%	• SEM: Surface erosion and fragmentation was observed. • NTA: The concentration/size distribution profiles confirmed the fragmentation of NPs to particles (<51 nm) and their aggregation. • Zeta potential: Less negative surface charge was obtained due to the protonation of introduced oxygen functional groups at neutral pH. • FTIR: The carbonyl index was increased. • XPS: The aromaticity of NPs decreased, and the structure gained more oxygen-based functional groups.	[67]

* This group synthesized metal-labeled PS NPs.
† Mineralization is monitored with TOC analysis.
§ The solution concentration was expressed as 0.9% (w/v), but the units (g L^{-1} or mg L^{-1}) were not specified.

3.1.1. Chemical oxidation

Among the chemical oxidation processes, ozonation is considered a robust AOP for the remediation of plastic particles in contaminated water [73,74]. The reactive agent, ozone (O_3), can attack electron-rich components such as activated aromatic rings, amines, and double bonds, resulting in ring opening and converting the complex compounds to smaller molecules. In addition, the $^{\bullet}OH$ produced during the ozonation process contributes significantly to the oxidation of toxic water pollutants [75,76]. Notably, pioneering studies have illustrated that ozonation is a valuable alternative for removing plastic fragments, proving that NPs break down into smaller molecules and gradually mineralize (Table 2) [26,68]. This can be attributed to three main reasons: i) O_3 introduces oxygen to the surface of NPs, enhancing the hydrophilicity and oxidative degradation; ii) the unsaturated and saturated bonds can be attacked directly by O_3 or indirectly by $^{\bullet}OH$ to open the aromatic rings and produce simple by-products [26]; iii) the produced by-products can undergo further reactions with the available reactive oxygen radical species, and convert to nontoxic compounds.

Li et al. [26] studied the ozonation and chlorination of PS NPs (100 nm) in pure water. In terms of analysis methods, gel permeation chromatography (GPC) followed the molecular weight of NPs during the reaction, while the efficiency of the degradation process was monitored by TOC analysis. Besides, modifications of the NPs were monitored by measuring the T_g of the polymeric particles and using SEM, FTIR, and XPS characterization methods. The generated intermediates during the ozonation process were followed by Pyr-GC/MS analysis. The SEM images (Fig. 3 (a-b)) depicted that after 240 min of ozonation, the size of the plastic particles reduced. The formation of polar functional groups was proved by the emerging peaks in FTIR, ascribed to the stretching vibration of carboxylic, alkyl hydroperoxide, and ketone groups, while the results of Pyr-GC/MS revealed seven oxygen-containing intermediates. Finally, the TOC was reduced by 42.7%,

indicating the successful mineralization of the NPs following this method. However, this study occurred in pure water and, thus, could not provide any information on the effect of other contaminants present in the degradation of NPs, like in actual contaminated water conditions.

Alternatively, Pulido-Reyes et al. [68] carried out a study on the degradation of NPs (Pd- labeled PS > 100 nm) in lake water via the ozonation process. In contrast to the previous work, in this research study, no changes were observed in the morphology of NPs (Figs. 3 (c-d)) after the ozonation process, as SEM and DLS indicated no agglomeration or fragmentation. Nonetheless, the surface charge, evaluated by zeta potential analysis, decreased with increasing ozone dose. On the top, through ICP-MS, it was confirmed that no Pd was released from the NPs during the ozonation process, proving that no degradation of NPs occurred, and this was mainly attributed to the use of high concentrations of NPs and the low reaction time.

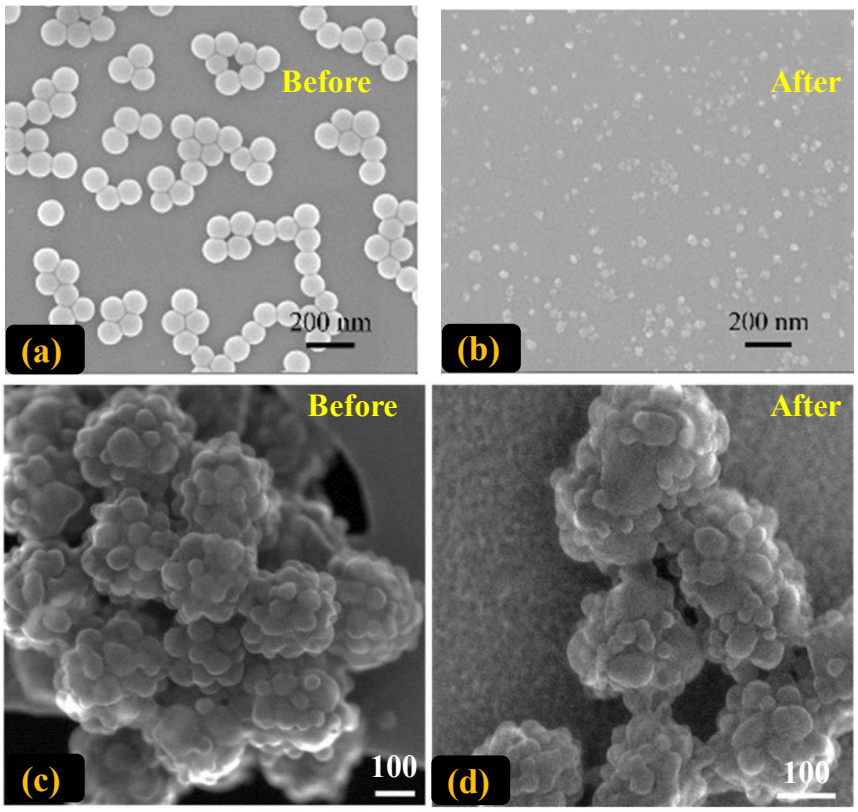

Fig 3. SEM images of PS NPs before (a) and after (b) 240 min of ozonation [26]. Secondary electron images of PS NPs before (c) and after (d) ozonation [68]. Reproduced with permission from the respective publishers.

3.1.2. Electrochemical oxidation

Electrochemical oxidation is another alternative method by which reactive oxygen species like $^{\bullet}OH$ and H_2O_2 are produced. It is an eco-friendly and cost-effective method to induce the degradation and mineralization of persistent pollutants [77,78]. Due to such advantages, this method has also been used to degrade NPs (Table 2).

Kiendrebeogo et al. [25] used the electro-oxidation (EO) and electro-peroxidation (EO-H_2O_2) methods to degrade 100 nm-sized PS NPs. Both methods selected boron-doped diamond (BDD) as an anode, and titanium and carbon felt (CF) were the cathodes. It has been demonstrated that in

the presence of Na_2SO_4 as the supporting electrolyte, a BDD anode can effectively oxidize sulfate ions to persulfate ($S_2O_8^{2-}$). This, in turn, plays a crucial role in the oxidation of organic compounds by generating sulfate radicals ($SO_4^{\bullet-}$), thereby facilitating the degradation process. As a result, their findings revealed that in both the EO and EO-H_2O_2 systems, hydroxyl radicals $^{\bullet}OH$ and $SO_4^{\bullet-}$ were generated. Furthermore, in the EO-H_2O_2 system, an additional generation of hydroxyl radicals $^{\bullet}OH$ and sulfate radicals $SO_4^{\bullet-}$ occurred, attributed to the decomposition of H_2O_2 and its direct interaction with the produced persulfate ions $S_2O_8^{2-}$. Hence, at the optimal conditions, the further generated reactive species during EO-H_2O_2 resulted in NPs degradation efficiency of 86.8% ± 1.8%, 2.6 times more than that obtained during the EO process. It is worth noting that the degradation efficiency was followed by monitoring the absorption peak of the PS C=C bonds at 254 nm. Moreover, it was confirmed that under optimal conditions, a significant portion of degraded NPs was mineralized (6.5 ± 0.64%) during the EO-H_2O_2 process.

3.1.3. Plasma-induced degradation processes

Electrical discharge plasma is one of the most promising AOPs, providing reactive oxidizing agents such as potential electrons and radicals ($^{\bullet}OH$) in situ via high voltage discharge. The generated reactive compounds can attack the chemical bonds of organic pollutants such as plastics and decay them into small and nontoxic molecules [79,80]. Zhou et al. [7] evaluated the performance of plasma-induced degradation of PS NPs (200 nm). According to the morphological analysis (Figs. 4 (a-b)), NPs were melted and rough after the treatment. The size and zeta potential variations were precisely studied using a nanoparticle potential analyzer. The findings depicted that in a brief time (15 min) (Fig. 4 (c)), the size of all NPs was decreased to 50-150 nm. Moreover, after the treatment, the zeta potential of NPs became more negative due to the hydroxyl and

carboxyl groups produced on their surface. Considering the FTIR, XPS, and fluorescence spectra presented in Figs. 4 (d-i), aliphatic groups were also created as hydroxylated and carboxylated byproducts.

Nonetheless, the degradation of NPs could also result in highly toxic byproducts, leading to secondary environmental pollution. Therefore, toxicity studies of the water where NPs were treated could offer a better insight into evaluating the performance of the NPs degradation process from a different point of view. To this aim, Zhou et al. [7] conducted a toxicity study to confirm the efficiency of the plasma-induced degradation process of NPs. Interestingly, in the presence of treated NPs with a concentration of 30 mg L^{-1}, the growth of *Scenedesmus obliquus*, a green algae species, was not significantly affected by the treated NPs. Notwithstanding, the toxicity effect of the treated NPs was substantially higher for the Human alveolar cells.

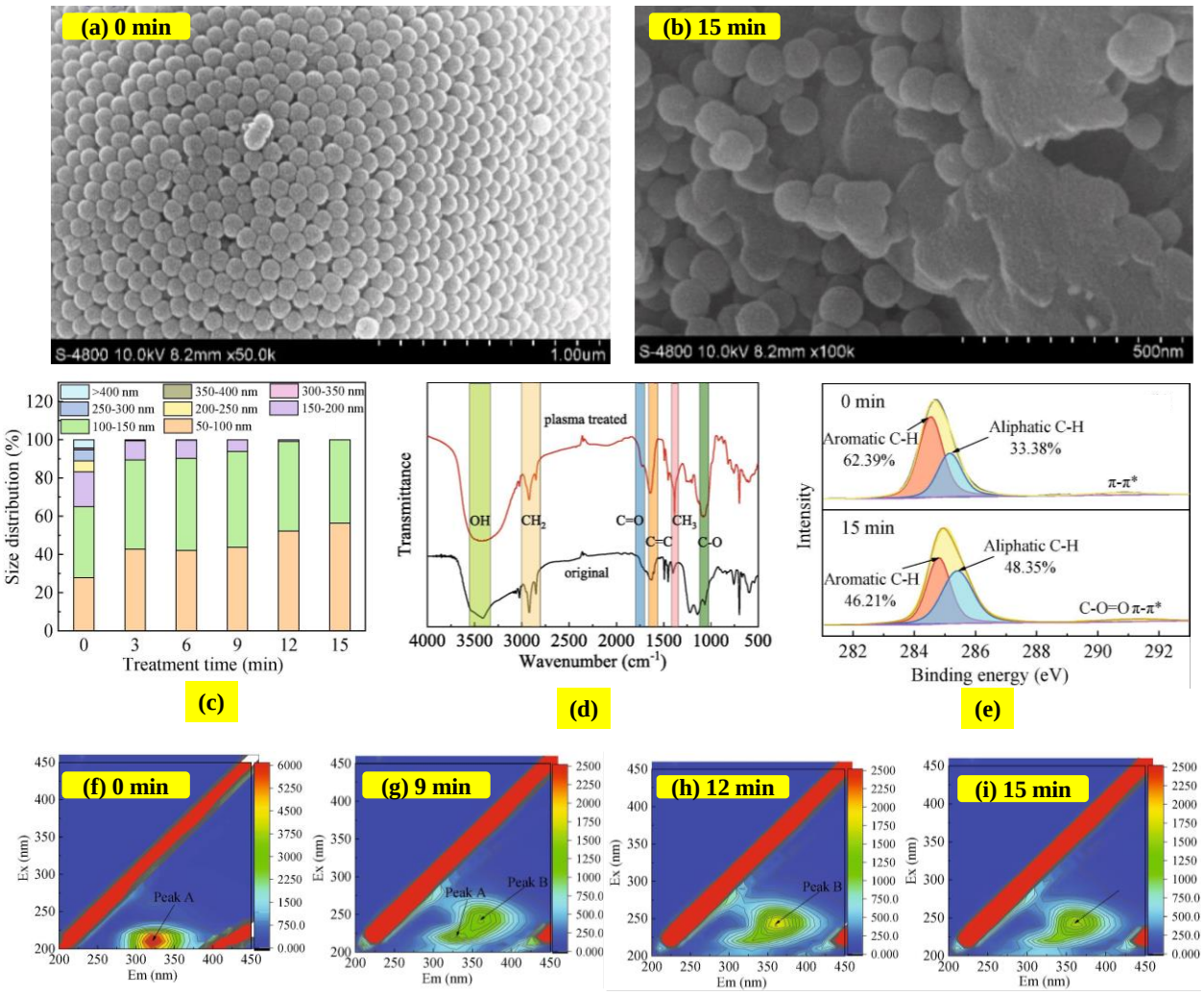

Fig. 4. (a-b) SEM images of PS NPS before and after 15 min of plasma-induced treatment. (c) Size distribution during the process. (d) FTIR and (e) high-resolution XPS spectra of C1s for pristine and treated NPs. (f-i) Recorded 3D fluorescence spectra of NPs in different time intervals [7]. Reproduced with permission from the publisher.

3.1.4. Photocatalytic process

Photocatalysis is a sustainable, cost-effective, widely available method and one of the most extensively used AOPs that deal with water purification, in line with the sustainable development

goals posed by the United Nations 2030 agenda [81]. In parallel with the other AOPs, photocatalysis was also applied to study the degradation of NPs (Table 2) [27–29] [69].

It is believed that when plastic is exposed to UV light, reactive radical species are produced, leading to chain decomposition and by-product generation. In this regard, Tian et al. [69] synthesized a ^{14}C-radioactively labeled PS (230 nm) and studied its phototransformation in water under UV irradiation (254 nm, 0.7 mW cm^{-2}). They proved that the UV irradiation of the NPs dispersed in nanopure water induced significant oxidation on the surface of the NPs as well as 17.1 % of mineralization in 48 h, while a substantial production of small-molecule oxidative products leached in the water. These hydrophilic products underwent further degradation or mineralization due to the UV irradiation. Nonetheless, according to the SEM images in Fig. 5 (a), the irradiation was not strong enough to induce any morphological changes in the NPs.

Furthermore, in a study by Cai et al. [71], various oxidants like NaClO and peroxymonosulfate (PMS) were subjected to UV irradiation to generate more reactive species such as $^{\bullet}OH$, $^{\bullet}Cl$, and $SO_4^{\bullet-}$, facilitating the efficient degradation of PS NPs. Their results showed that the UV/PMS process exhibited superior performance. The UV/PMS system achieved 94.30% turbidity removal and 63.90% mineralization in 360 minutes, while UV/NaClO showed 78.20% turbidity removal and 7.00% mineralization. As depicted in Fig. 5 (b), almost no spherical particles were observed after degradation. Surprisingly, the untreated PS NPs exhibited low toxicity, with just a 1.98% inhibition rate on luminescent bacteria, contrary to the ones subjected to the degradation process (98.19%). This indicates that despite the effective degradation of NPs, the resulting by-products are more toxic. Consequently, it is essential to devise a robust degradation method that breaks down solid NPs and efficiently mineralizes any potential by-products resulting from NP chain cleavage.

Luca et al. [70] explored the feasibility of an alternative homogeneous photocatalytic system based on the Fenton reaction. In the photo-Fenton process ($UV/H_2O_2/Fe^{3+}$), H_2O_2 and Fe^{3+} undergo reactions under UV irradiation, generating further $^{\bullet}OH$ radicals. Under the optimal condition reported in Table 2, the mineralization efficiency followed the trend: $UV/H_2O_2/Fe^{3+} > UV/H_2O_2 > H_2O_2/Fe^{3+}$ > photolysis, underscoring the significance of additional $^{\bullet}OH$ production in the degradation of NPs. The turbidity, TOC, and TEM analyses confirmed the thorough degradation and mineralization of PS NPs after 60 min of the photo-Fenton process ($UV/H_2O_2/Fe^{3+}$). In addition, TEM images revealed that the size of PS NPs decreased during the degradation process. Despite the total mineralization observed, the use of UV as the light source and the homogeneous addition of iron (II) sulfate heptahydrate and H_2O_2 in the reaction media may limit the applicability of this process for degrading water pollutants, including NPs.

Heterogeneous photocatalytic processes require a semiconductor that possesses a void energy region between the top of the valence band (VB) and the bottom of the conduction band (CB), called energy band gap, Eg. Generally, the semiconductor catalysts are activated through the absorption of a photon with higher energy than the E_g to induce the promotion of an electron from the VB to the CB, leaving behind a hole in the VB. The photogenerated electron and hole can oxidize water to hydroxyl radicals or reduce oxygen to superoxide radicals. The produced radical species can then oxidize the nearby organic compounds like plastic particles. Various heterogeneous photocatalysts, including films (TiO_2 [27], Cu_xO [28], and MOF-derived porous α-Fe_2O_3 [65]), foams (TiO_2– P25/β- SiC [29,66]), TiO_2/MOF(MIL-100(Fe) particles immobilized on perlite granules [72], and SnO_2/g-C_3N_4 [67] immobilized on the electrospun vinylidene fluoride-co-hexafluoropropylene, were used to degrade different NP types (such as PS, PET, and Polymethylmethacrylate) in the 120-500 nm size range. Fig. 5 depicts the heterogeneous

photocatalytic systems like TiO_2/β-SiC foams, MOF-derived Fe_2O_3 film, and SnO_2/g-C_3N_4/PVDF-HFP composite. Turbidity, TOC, GC-MS, FTIR, XPS, FE-SEM, TEM, NTA, and fluorescence spectroscopy analyses were conducted in the mentioned studies to follow the PS NPs degradation during the photocatalytic process.

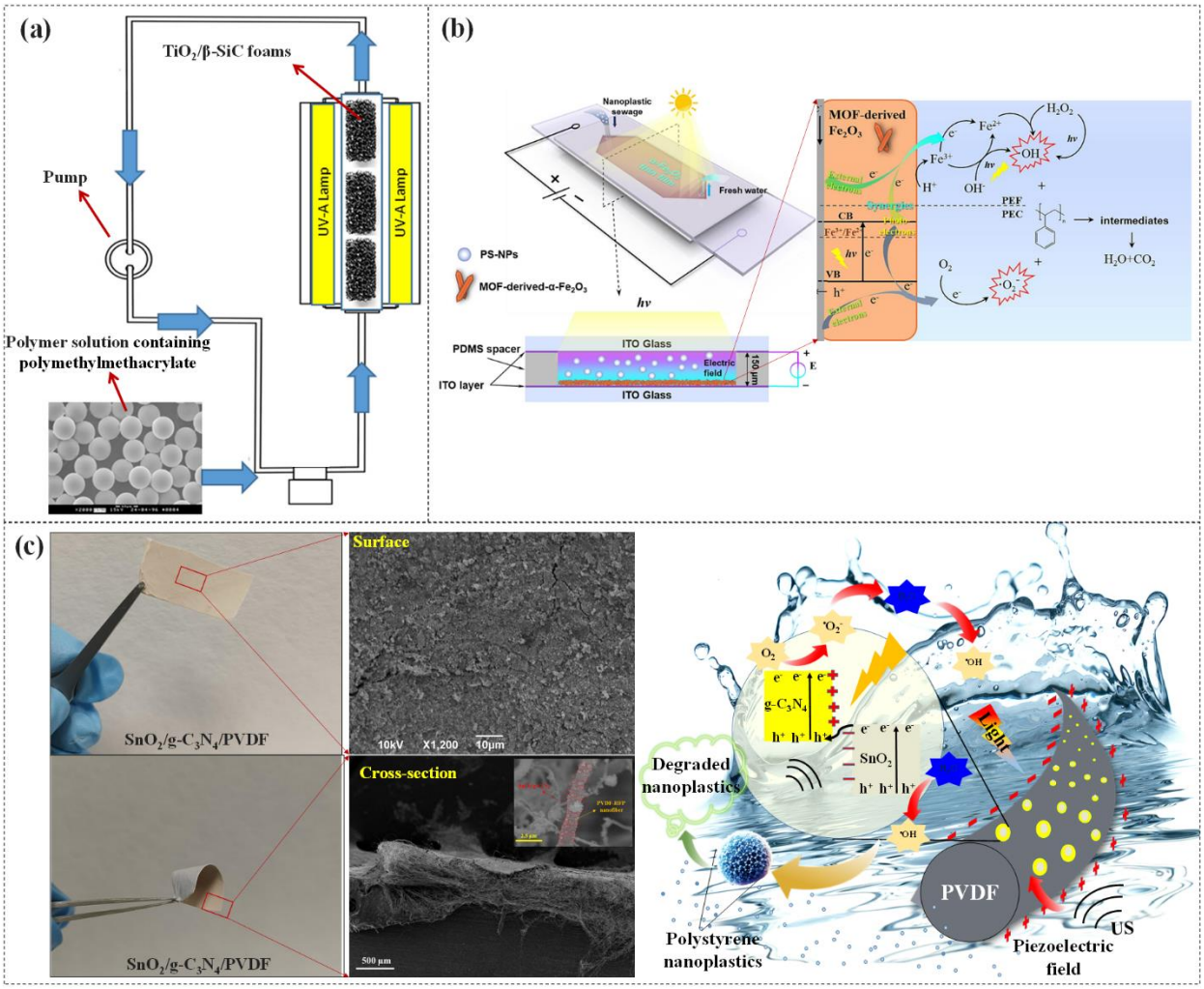

Fig. 5. Overview of heterogeneous photocatalytic systems used to degrade nanoparticles (NPs). (a) Photocatalytic tubular reactor incorporating TiO_2/β-SiC foams [29]. (b) Microreactor featuring a MOF-derived Fe_2O_3 film, including a schematic representation of the photoelectro-Fenton

mechanism [65]. (c) SnO_2/g-C_3N_4/PVDF-HFP composite, along with its piezo-photocatalytic mechanism [67]. Reproduced with permission from the respective publishers.

In particular, under UV irradiation, TiO_2-based photocatalysts, especially in the mixed (nanotubes/nanograss) structure, resulted in 12.7% of mineralization [27]. As revealed by the FTIR analysis of the PS NPs after the photocatalytic process, the introduction of oxygen to the structure of NPs and generating new functional groups like carbonyl and ketone can affect the process. The peak is attributed to the carbonyl group, and a reference peak is used to calculate the carbonyl index (CI). For the mixed TiO_2 structure under UV irradiation, the CI was increased from 0.08 to 0.27. This increase suggests introducing additional oxygen-based functional groups to the organic polymeric chains, promoting chain scission and subsequent degradation or mineralization. Furthermore, Allé et al. [29] proved that 7 h of UVA irradiation in the presence of TiO_2– P25/β-SiC foams can cause the polymethylmethacrylate NPs mineralization with an efficiency of 50%, indicating that such components are highly promising in the NPs remediation field. Upon detailed evaluation of the effects of various experimental parameters such as the flow rate, the initial pH, and the UV light intensity on the NPs photodegradation efficiency, it can be concluded that the higher the NPs residence in the reactor (low flow rate) the higher degradation efficiency was achieved, while the higher the UV light intensity, the higher the reaction kinetic rate constant, therefore the faster is the photodegradation process. On the other hand, the primary solution (pH>9) showed a negative effect on the photodegradation, with the mineralization efficiency reaching 17%, due to the repulsion force between the negatively charged surface of TiO_2 and the negatively charged carboxylate groups of the polymethylmethacrylate NPs. In addition, the same research group conducted a methodological study [66] to explore the impact of powdery or

immobilized TiO_2 on the reliability of characterization methods. They extensively discussed the suitable analytical tools for qualitatively and quantitatively tracking the degradation of NPs with different sizes (140, 300, and 508 nm). Their results for each reaction mode are summarized in Table 2. Employing commercially available Aeroxide TiO_2 P25 in powdery form for batch slurry reactions and upon immobilization on β-SiC foams, they found that the presence of TiO_2 particles in the slurry hindered monitoring of degraded NPs using TOC, UV-Vis, or Py-GC/MS analyses. Conversely, in the immobilized mode, the collected suspension after photocatalytic degradation allowed for reliable analyses. Moreover, FE-SEM, TEM, and DLS provided indications of NPs degradation during reactions, and the batch slurry mode yielded unreliable and non-quantitative results. Hence, while immobilizing photocatalysts may decrease the interaction with NPs, this remains the most effective strategy for a reliable characterization in NPs degradation studies.

Despite advances in heterogeneous photocatalytic degradation of NPs, the reported systems predominantly rely on UV light sources, which cover only a small portion of sunlight. Therefore, further studies are needed for a sustainable transit toward effective NPs remediation without the exclusive need for UV light. In this regard, Acuña-Bedoya et al. [28] developed a photocatalyst active under sunlight irradiation composed of immobilized copper oxide semiconductors grown through the anodizing process in NH_4F media. They studied the degradation of PS NPs under visible light irradiation (Table 2). The reaction process results in a CI increase from 0.70 to 59.75 after 50 hours, which, together with the GC/MS analysis, proves the formation of carbonyl groups in the structure of NPs. Furthermore, 23.5% and 15% of NPs degradation and mineralization were observed. Combinations between different semiconductors have been explored to improve the performance of the photocatalysts under daylight irradiation. In particular, metal-organic frameworks (MOFs) composed of Fe(III) metal centers linked with 1,3,5-benzene tricarboxylic

acid were employed to boost the photocatalytic performance of TiO_2 [72]. These MOFs enhanced the absorption of simulated solar light and promoted the transfer of photoexcited electrons to the metal clusters. The resulting final composite was immobilized onto porous perlite mineral particles, and its ability to degrade PET NPs was assessed. Compared to pure TiO_2, the composite with MOF exhibited improved NPs degradation performance validated across multiple parameters. Specifically, the CI increased from 0.96 to 0.99, indicating superior photocatalytic activity. This, in combination with the decrease in the turbidity ratio of the NPs dispersion (final/initial) reaching 0.454 for TiO_2/MOF, while for pure TiO_2 was 0.539, highlights the superior performance of TiO_2/MOF in the degradation of NPs under solar light irradiation. However, as highlighted by the authors, the released soluble organic compounds pose a higher toxicity risk during the degradation process than the NPs themselves. Moreover, the developed process showed optimal performance at a solution pH of 3, which may not accurately represent the pH levels found in natural water samples. Alternatively, this pH deviation could compromise the stability of the photocatalysts and potentially result in the leaching of elements from the applied MOF into the reaction medium, thereby shifting the photocatalytic process from heterogeneous to homogeneous.

To further enhance the performance of the systems for the degradation of NPs under daylight irradiation, a recent study focused on the combination of photocatalytic and piezocatalytic activity. In particular, a Z-scheme piezo-photocatalyst (SnO_2/g-C_3N_4/PVDF-HFP) was developed, capable of using solar and water-driven energy sources to degrade PS NPs. This catalyst shows strong solar light absorption, notable piezoelectricity, and ease of recovery. The efficacy of the piezo-photocatalytic process in oxidizing and fragmenting PS NPs was demonstrated using various characterization techniques, including SEM, NTA, XPS, FTIR, and TOC. As outlined in Table 2, the piezo-photocatalytic experiments produced reactive species that oxidized the NPs, resulting in

their fragmentation and decreased aromaticity. Through this strategy, 46% mineralization was achieved within 15 hours of interaction.

Overall, the reported studies represent meaningful progress in NPs degradation by leveraging renewable energy sources, including a broad spectrum of solar light beyond just UV radiation. However, to further enhance practical feasibility and ensure broader applicability, it is crucial to assess and optimize the performance of these processes within the varied and challenging conditions presented by complex environmental samples.

In addition to engineering an appropriate photocatalyst, reactors play a crucial role in photocatalytic degradation performance. Optofluidic catalytic reactors offer advantages such as a large specific surface area, high mass transfer, and photon utilization efficiency and have been reported to enhance the removal efficiency of soluble water pollutants [65]. In the case of NPs, Chen et al. [65] introduced a photoelectron-Fenton microreactor to degrade PS NPs. They synthesized a MOF-derived porous α-Fe_2O_3 thin film and coated it in the reaction chamber to facilitate Fenton reactions. Under low pH conditions, available H_2O_2 and leached Fe^{2+} from α-Fe_2O_3 initiated Fenton reactions, producing $^{\bullet}OH$ and Fe^{3+}. Additionally, electrons and holes were generated through the light absorption of α-Fe2O3. The photogenerated electrons could combine with Fe^{3+} to regenerate Fe^{2+} for further Fenton reactions, leading to the continuous production of $^{\bullet}OH$ for attacking NPs in water. Their designed photo-reactor achieved over 80% degradation, monitored through the turbidity reduction of the PS NPs dispersion in water under 1.2 V bias and 120 mW cm^2 of simulated solar irradiation. While this is a well-performant process, no information was provided on the mineralization of potential by-products. Furthermore, similar to other studies, the reaction conditions do not accurately reflect the complexity of real-world environmental samples, where various types of environmentally relevant NPs are present in complex organic matrices.

In conclusion, researchers have endeavored to enhance the sustainability, feasibility, and performance of photo-based NP degradation processes. While acknowledging variations in reaction conditions and analytical methods employed for assessing degraded NPs, a common trend emerges: NPs undergo significant morphological modifications during photo-based treatments. The SEM analyses (summarized in Fig. 6) underscore, contrary to the limited efficacy of photolysis (Fig. 6(a)), where merely surface cracks on NPs are induced. However, in the photocatalytic processes, a significant NP degradation with evident size reduction (Figs. 6(b-c)), creation of cavities on the NPs surface, and fragmentation (Figs. 6 (d-e)) occurs. However, these results indicate that more than current photo-based processes may be needed for thorough NP degradation. The cleavage of polymeric chains could lead to the formation of smaller fragments, potentially generating more toxic by-products and posing more significant environmental challenges than the original NPs. To address this, comprehensive studies are needed, encompassing the morphological and chemical analyses of NPs, the reaction media, and toxicological assessments of the potential by-products. Such endeavors would significantly enhance our understanding of the effectiveness of photo-based processes in the remediation of sustainable NPs.

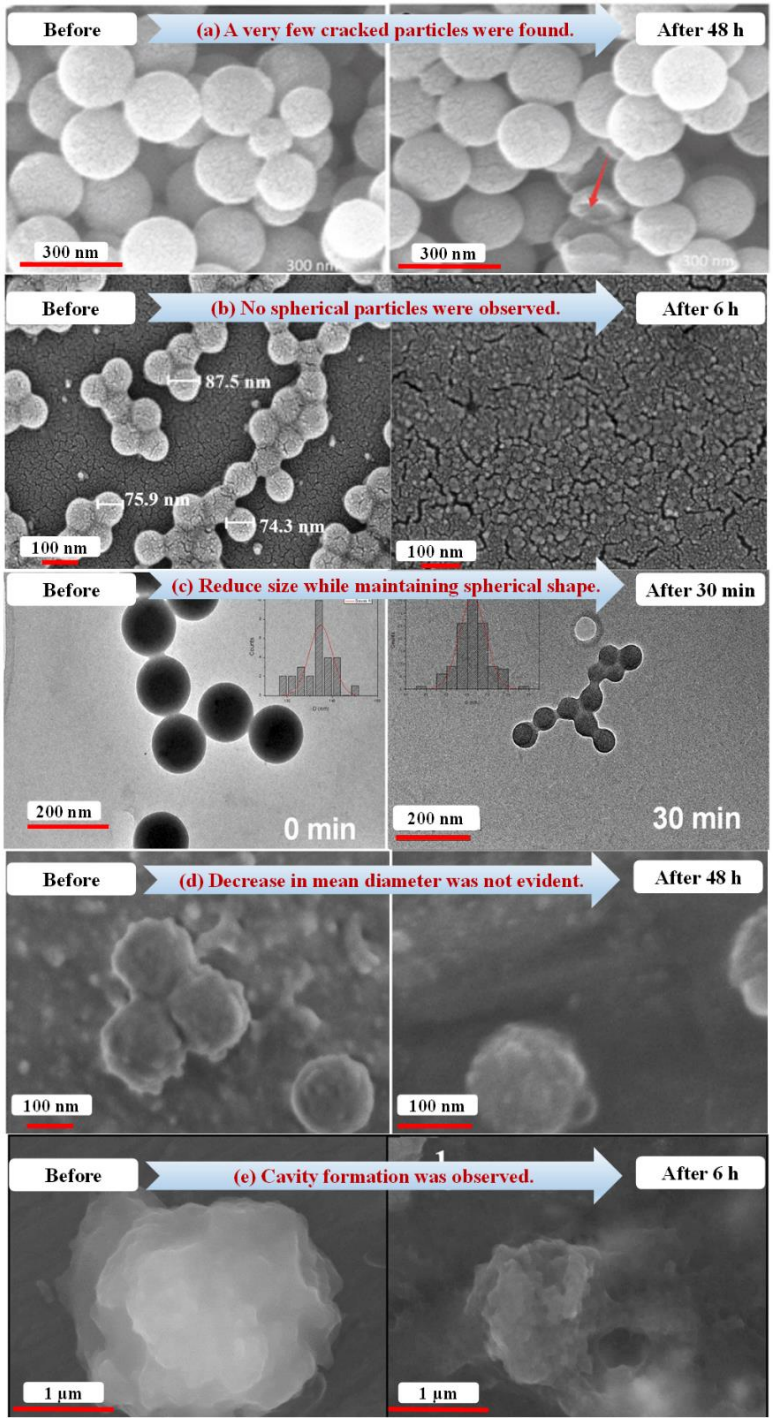

Fig 6. SEM/TEM images of pure and degraded PS NPs during photo-based processes. (a) UV irradiation [69] (b and c) homogenous photocatalytic processes [70,71], and (d and e) heterogeneous photocatalytic processes [66,72]). Reproduced with permission from the respective publishers.

4. Current research gaps and perspectives in degrading NPs through AOPs

While various AOPs have been utilized for the degradation of NPs, these endeavors encounter certain limitations that must be addressed for a more viable and effective NPs degradation approach. Based on the literature review, we highlight the most evident shortcomings encountered alongside the appropriate methods that may be considered to address these issues.

4.1. Overlooked challenges stemming from the complex environment

Most of the studies on the NPs environmental fate and their remediation approaches are performed using monodispersed artificial nanobeads, mostly PS NPs, at high concentrations far from the environmentally relevant ones. However, these conditions do not usually represent the various types of NPs present in the environment and their expected concentration and, therefore, do not reflect real-world exposure. These plastic nanostructures mainly possess few defects and homogeneous chemical composition, substantially different from the NPs dispersed in the environment. These have irregular shapes and complex surface chemistry due to the degradation experienced. This raises questions about the accuracy and reliability of the obtained results [51]. Hence, for a more accurate assessment of NPs' environmental implications, it is essential to use more environmentally relevant media or gather them directly from their natural surroundings.

Estimations on the environmental concentration of NPs indicate that it is very low (1 pg L^{-1} - 15 μg L^{-1} for NPs of 50nm [82]). At the same time, they may be embedded in complex organic matrices, making their collection and quantification extremely difficult. Before being characterized or quantified, liquid samples should be processed with various pretreatment steps to separate the NPs from their complex organic matrices [51,83]. On the other hand, due to the deficient environmental concentrations of the NPs, much lower than the detection limit of some characterization techniques, pre-concentration methods such as ultrafiltration, centrifuge, cloud point extraction, and freeze-drying should be applied before the proper characterization [84–86].

Confronted with the complexities of collecting and processing environmental samples, scientists have sought alternative approaches to mimic environmentally relevant NPs through the mechanical and photocatalytic degradation of larger plastic fragments. Employing various top-down methodologies such as laser ablation [87] and ball milling [88], these efforts have resulted in the fabrication of NPs with properties closely resembling those found in natural environments. However, despite this achievement, such approaches have predominantly been utilized for toxicological evaluations and have seen limited integration into NP degradation through AOPs.

Moreover, wastewater is replete with diverse organic and inorganic compounds, which can impede the efficiency of water pollutant degradation processes [89]. NPs are solid water pollutants characterized by their small size and high surface area. Hence, in real-world environmental samples, NPs are rarely pristine; they often harbor various organic and inorganic components sorbed on their surface [90]. In addition, environmental samples typically contain different NP types. These factors pose significant constraints on the feasibility of degradation processes. While the effects of environmental factors like pH variations, water complexity, and the presence of ions and organic compounds on degrading water-soluble pollutants have been studied, there is still a significant gap in understanding how these factors affect NP degradation [89,91].

4.2. Limitations in characterizing NPs after AOPs

Regrettably, there is still a lack of reliable analytical techniques that are both straightforward and sensitive enough to detect individual plastic particles (< 1 μm) from complex mixtures of various polymers, additives, and degradation products. This makes their analysis even more challenging. Most of the so-far reported characterization techniques for NPs are presented in Fig. 7. Specifically, SEM, TEM, DLS, zeta potential, FTIR, and XPS are widely used techniques for

studying the morphology, size distribution, shape, and surface charge, as well as the chemical composition of the degraded NPs [92]. However, such analyses can be challenging due to their low resolution and high detection limit, which demand high NPs concentrations, but also due to the NPs agglomeration and low particle size, limiting their applicability in some instances [33,49]. Due to these constraints, advanced technological solutions should be adopted to study the degradation of NPs.

Recent advancements in NP characterization, rarely considered for AOPs, could prove invaluable for addressing such challenges in future studies. For instance, confocal laser scanning microscopy (CLSM) offers a non-destructive approach to analyzing the size, shape, and distribution of NPs in complex matrices [93]. The advanced optical nanoscope (NOMON) uses a super-resolution lens to enhance resolution and image quality, enabling detailed characterization of NPs in water [49]. NTA provides valuable insights into size distribution, shape, and concentration by analyzing individual particles [94]. In addition, near-edge X-ray absorption exemplary spectra (NEXAFS) are a powerful tool that can be used to investigate the chemical and structural properties of plastic particles that are less than 100 nm in size [95]. In contrast to FTIR, which is more appropriate for larger particle sizes with high particle concentrations and polar functional groups, Raman spectroscopy, including surface-enhanced Raman spectroscopy (SERS), provides chemical fingerprint identification with exceptional sensitivity, allowing for the analysis of nanoparticles at low concentrations [96,97]. Furthermore, for analyzing the emergence of various intermediates during the degradation processes, Pyr-GC/MS and fluorescent spectroscopy were employed. These methods are sensitive to impurities and possess high detection limits. Hence, pretreatment and concentration of the NP samples are necessary [98]. However, the thermal

desorption-proton transfer reaction-mass spectrometry (TD-PTR-MS) was appropriate for the characterization of NPs at lower concentrations and in natural environments [99].

In addition to these methods, established combined techniques can further enhance the simultaneous morphological and chemical analysis, increasing the accuracy of results when studying the degradation of NPs in real-world samples [14,15]. For instance, Raman spectroscopy can be integrated with microscopy (μ-Raman spectroscopy) to identify NPs at a minimum size of 1 μm [100]. Furthermore, Raman spectroscopy integrated with optical tweezers known as the Raman tweezers (RTs) can trap and characterize plastics in the range of < 1 μm even in seawater [98,100]. Nano-FTIR and visible-near infrared dark-field hyperspectral imaging (DF-HSI) combine microscopy with spectroscopy, allowing imaging and chemical identification of various plastic particles with sizes less than 1000 nm [101,102]. Scanning transmission X-ray microscopy (STXM) combines the merits of X-ray microscopy and near-edge X-ray absorption fine structure spectroscopy (NEXAFS). It can be used for the chemical analysis of NPs [95]. Separation techniques like field-flow fractionation (F3) and asymmetric flow field-flow fractionation (AF4) enable the isolation of particles based on physical characteristics, facilitating comprehensive analysis of particle interactions in complex environments [103].

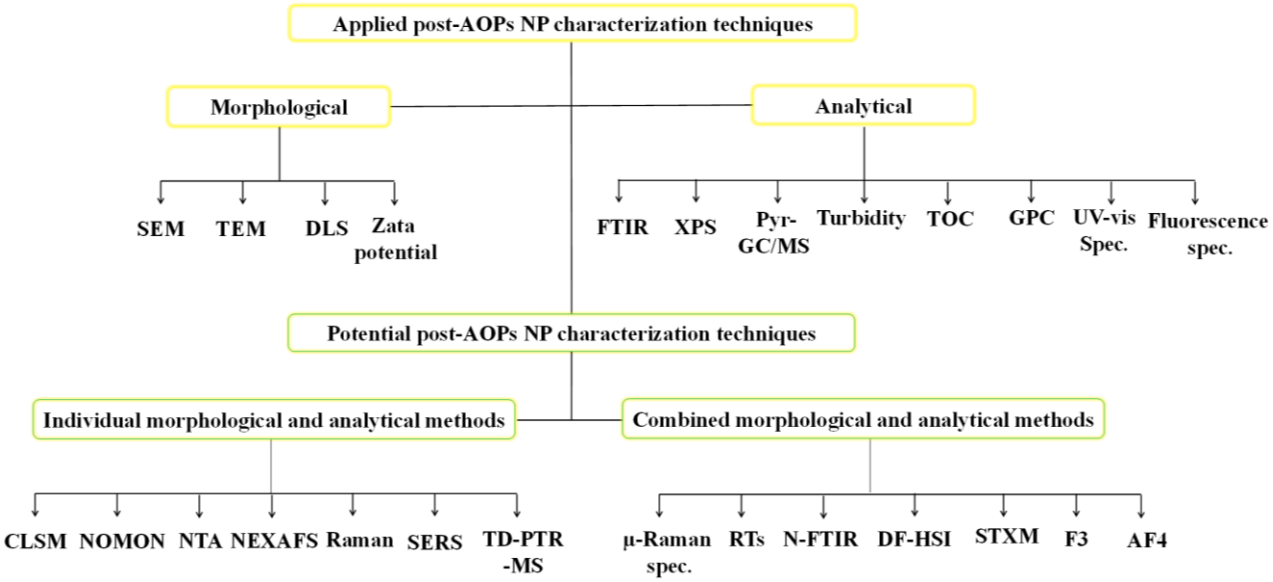

Fig. 7. Overview of characterization methods utilized and potentially beneficial for analyzing degraded NPs through AOPs.

In conclusion, the study of NP degradation through AOPs is still in its early stages, and it is unsurprising if the points mentioned here cover only some of the research gaps in this field. Moreover, current AOPs often need complete NP elimination and mineralization, necessitating chemical additives, UV light sources, and extended reaction times. Hence, they may inadvertently lead to secondary water pollution and increased energy consumption. Furthermore, given that NPs act as insoluble water contaminants, developing efficient reactors and highly effective immobilized heterogeneous catalytic systems is imperative. Optimization of these systems is essential for maximizing NP-catalyst interactions while minimizing energy and chemical usage during catalyst recovery [65,66]. Bridging these knowledge gaps is crucial for devising more effective and sustainable strategies to mitigate NP contamination in water systems.

5. Conclusion

NPs from primary and secondary sources find their way to enter the water bodies. The detected NPs in drinking water, even of low concentration, led to concerns about their potential hazards. Although various conventional methods were applied for the degradation of NPs from water, their complexity and inadequacy in the total degradation and mineralization limit their wide application. AOPs are the alternative methods that can produce reactive radical species to degrade NPs to small and harmless compounds. Considering the efficiency of these methods, several heterogeneous and homogenous AOPs were applied to the degradation of plastic micro and nanofragments. As reported, ozonation, electro-oxidation, electro-peroxidation, plasma-induced, and photocatalytic processes showed an effective performance for the degradation of NPs. Nonetheless, considering the slow publication rate in applying AOPs for the in situ degradation of NPs, this emerging field remains in its infancy, necessitating more significant effort to explore robust AOPs with improved efficiency and minimal environmental impact.

Moreover, existing research primarily involves artificial NPs and controlled environmental conditions, highlighting the crucial need for investigations using environmentally realistic NP samples under potentially posing conditions. This review reveals that sample preparation for various characterization techniques needs to be more specific, underscoring the importance of providing precise experimental and analytical details. Coordinated efforts are therefore essential to enhance experimental protocols and address remaining challenges. This collective endeavor will foster a deeper understanding of NP degradation via AOPs, paving the way for sustainable and effective NP remediation, even on an industrial scale.

References

[1] V. Percec, Q. Xiao, *Chem* **2020**, *6*, 2855.

[2] Q. Liu, Z. Chen, Y. Chen, F. Yang, W. Yao, Y. Xie, *J. Agric. Food Chem.* **2021**, *69*, 10450.

[3] J. Domenech, C. Cortés, L. Vela, R. Marcos, A. Hernández, *Biomolecules* **2021**, *11*, 859.

[4] S. Kahlert, C. R. Bening, *Resour. Conserv. Recycl.* **2022**, *181*, 106279.

[5] "The New Plastics Economy: Rethinking the future of plastics," can be found under https://ellenmacarthurfoundation.org/the-new-plastics-economy-rethinking-the-future-of-plastics, **n.d.**

[6] "Global plastic production," can be found under https://www.statista.com/statistics/282732/global-production-of-plastics-since-1950/, **n.d.**

[7] L. Zhou, R. Wang, Y. Liu, Y. Zhang, J. Zhou, G. Qu, S. Tang, T. Wang, *Chem. Eng. J.* **2022**, *433*, 134543.

[8] O. S. Alimi, J. Farner Budarz, L. M. Hernandez, N. Tufenkji, *Environ. Sci. Technol.* **2018**, *52*, 1704.

[9] K. L. E. Berry, N. Hall, K. Critchell, K. Chan, B. Bennett, M. Mortimer, P. J. Lewis, in *Mar. Pollut. – Monit. Manag. Mitig.* (Ed.: A. Reichelt-Brushett), Springer Nature Switzerland, Cham, **2023**, pp. 207–228.

[10] A. A. Mohana, S. M. Farhad, N. Haque, B. K. Pramanik, *Chemosphere* **2021**, *284*, 131430.

[11] N. B. Hartmann, T. Hüffer, R. C. Thompson, M. Hassellöv, A. Verschoor, A. E. Daugaard, S. Rist, T. Karlsson, N. Brennholt, M. Cole, M. P. Herrling, M. C. Hess, N. P. Ivleva, A. L. Lusher, M. Wagner, *Environ. Sci. Technol.* **2019**, *53*, 1039.

[12] S. M. O'Neill, J. Lawler, *Case Stud. Chem. Environ. Eng.* **2021**, *3*, 100091.

[13] J. Domenech, M. de Britto, A. Velázquez, S. Pastor, A. Hernández, R. Marcos, C. Cortés, *Biomolecules* **2021**, *11*, 1442.

[14] I. Ali, Q. Cheng, T. Ding, Q. Yiguang, Z. Yuechao, H. Sun, C. Peng, I. Naz, J. Li, J. Liu, *J. Clean. Prod.* **2021**, *313*, 127863.

[15] S. M. Patil, N. R. Rane, P. O. Bankole, P. Krishnaiah, Y. Ahn, Y.-K. Park, K. K. Yadav, M. A. Amin, B.-H. Jeon, *Chem. Eng. J.* **2022**, *430*, 132913.

[16] A. S. I. Abdoul Magid, Md. S. Islam, Y. Chen, L. Weng, J. Li, J. Ma, Y. Li, *Sci. Total Environ.* **2021**, *784*, 147115.

[17] Y. Gong, Y. Bai, D. Zhao, Q. Wang, *Water Res.* **2022**, *208*, 117884.

[18] Y. Zhang, A. Diehl, A. Lewandowski, K. Gopalakrishnan, T. Baker, *Sci. Total Environ.* **2020**, *720*, 137383.

[19] Z. Chen, C. Chen, X. Luo, J. Liu, Z. Huang, *Appl. Clay Sci.* **2021**, *213*, 106264.

[20] Z. Chen, Z. Huang, J. Liu, E. Wu, Q. Zheng, L. Cui, *J. Hazard. Mater.* **2021**, *406*, 124697.

[21] Z. Chen, J. Liu, C. Chen, Z. Huang, *Chemosphere* **2020**, *252*, 126450.

[22] *Sci. Total Environ.* **2021**, *773*, 145111.

[23] R. Wang, L. Zhang, B. Chen, X. Zhu, *J. Membr. Sci.* **2020**, *614*, 118470.

[24] M. Shen, B. Song, C. Zhou, T. Hu, G. Zeng, Y. Zhang, *Sci. Total Environ.* **2022**, *842*, 156723.

[25] M. Kiendrebeogo, M. R. Karimi Estahbanati, Y. Ouarda, P. Drogui, R. D. Tyagi, *Sci. Total Environ.* **2022**, *808*, 151897.

[26] Y. Li, J. Li, J. Ding, Z. Song, B. Yang, C. Zhang, B. Guan, *Chem. Eng. J.* **2022**, *427*, 131690.

[27] L. P. Domínguez-Jaimes, E. I. Cedillo-González, E. Luévano-Hipólito, J. D. Acuña-Bedoya, J. M. Hernández-López, *J. Hazard. Mater.* **2021**, *413*, 125452.

[28] J. D. Acuña-Bedoya, E. Luévano-Hipólito, E. I. Cedillo-González, L. P. Domínguez-Jaimes, A. M. Hurtado, J. M. Hernández-López, *J. Environ. Chem. Eng.* **2021**, *9*, 106208.

[29] P. H. Allé, P. Garcia-Muñoz, K. Adouby, N. Keller, D. Robert, *Environ. Chem. Lett.* **2021**, *19*, 1803.

[30] Y. Zhang, F. Cheng, T. Zhang, C. Li, J. Qu, J. Chen, W. J. G. M. Peijnenburg, *Environ. Sci. Technol.* **2022**, *56*, 3085.

[31] A. Kundu, N. P. Shetti, S. Basu, K. Raghava Reddy, M. N. Nadagouda, T. M. Aminabhavi, *Chem. Eng. J.* **2021**, *421*, 129816.

[32] B. K. Pramanik, S. K. Pramanik, S. Monira, *Chemosphere* **2021**, *282*, 131053.

[33] S. Gangadoo, et al., *Sci. Total Environ.* **2020**, *732*, 138792.

[34] S. Lambert, M. Wagner, *Chemosphere* **2016**, *145*, 265.

[35] S. Prenner, A. Allesch, M. Staudner, M. Rexeis, M. Schwingshackl, M. Huber-Humer, F. Part, *Environ. Pollut.* **2021**, *290*, 118102.

[36] M. Mathissen, V. Scheer, R. Vogt, T. Benter, *Atmos. Environ.* **2011**, *45*, 6172.

[37] A. L. Dawson, S. Kawaguchi, C. K. King, K. A. Townsend, R. King, W. M. Huston, S. M. Bengtson Nash, *Nat. Commun.* **2018**, *9*, 1001.

[38] L. Peng, D. Fu, H. Qi, C. Q. Lan, H. Yu, C. Ge, *Sci. Total Environ.* **2020**, *698*, 134254.

[39] W. C. Li, H. F. Tse, L. Fok, *Sci. Total Environ.* **2016**, *566–567*, 333.

[40] C.-B. Jeong, H.-M. Kang, Y. H. Lee, M.-S. Kim, J.-S. Lee, J. S. Seo, M. Wang, J.-S. Lee, *Environ. Sci. Technol.* **2018**, *52*, 11411.

[41] J. Bhagat, N. Nishimura, Y. Shimada, *J. Hazard. Mater.* **2021**, *405*, 123913.

[42] M. Mofijur, et al., *Environ. Res.* **2021**, *195*, 110857.

[43] M. Cole, P. Lindeque, E. Fileman, C. Halsband, R. Goodhead, J. Moger, T. S. Galloway, *Environ. Sci. Technol.* **2013**, *47*, 6646.

[44] Y. M. M. Paing, Y. Eom, G. B. Song, B. Kim, M. G. Choi, S. Hong, S. H. Lee, *Sci. Total Environ.* **2024**, *924*, 171681.

[45] M. C. González-Caballero, et al., *Chemosphere* **2024**, *355*, 141815.

[46] Marfella Raffaele, et al., *N. Engl. J. Med.* **2024**, *390*, 900.

[47] Y. Li, Z. Wang, B. Guan, *Environ. Res.* **2022**, *204*, 112134.

[48] M. Kosuth, S. A. Mason, E. V. Wattenberg, *PLOS ONE* **2018**, *13*, e0194970.

[49] Y. Huang, K. K. Wong, W. Li, H. Zhao, T. Wang, S. Stanescu, S. Boult, B. van Dongen, P. Mativenga, L. Li, *J. Hazard. Mater.* **2022**, *424*, 127404.

[50] Y. Liu, Y. Hu, C. Yang, C. Chen, W. Huang, Z. Dang, *Water Res.* **2019**, *163*, 114870.

[51] H. Cai, E. G. Xu, F. Du, R. Li, J. Liu, H. Shi, *Chem. Eng. J.* **2021**, *410*, 128208.

[52] Z. A. Ganie, N. Khandelwal, E. Tiwari, N. Singh, G. K. Darbha, *J. Hazard. Mater.* **2021**, *417*, 126096.

[53] E. Tiwari, N. Singh, N. Khandelwal, F. A. Monikh, G. K. Darbha, *J. Hazard. Mater.* **2020**, *397*, 122769.

[54] R. Amanna, M. Samavi, S. K. Rakshit, in *Curr. Dev. Biotechnol. Bioeng.* (Eds.: R. D. Tyagi, A. Pandey, P. Drogui, B. Yadav, S. Pilli), Elsevier, **2023**, pp. 293–314.

[55] G. Zhou, X. Huang, H. Xu, Q. Wang, M. Wang, Y. Wang, Q. Li, Y. Zhang, Q. Ye, J. Zhang, *Sci. Total Environ.* **2022**, *820*, 153190.

[56] H. Zhao, X. Huang, L. Wang, X. Zhao, F. Yan, Y. Yang, G. Li, P. Gao, P. Ji, *Chem. Eng. J.* **2022**, *430*, 133122.

[57] N. Zhu, Q. Yan, Y. He, X. Wang, Z. Wei, D. Liang, H. Yue, Y. Yun, G. Li, N. Sang, *J. Hazard. Mater.* **2022**, *433*, 128756.

[58] A. Gabet, C. Guy, A. Fazli, H. Métivier, C. de Brauer, M. Brigante, G. Mailhot, *Sep. Purif. Technol.* **2023**, *317*, 123877.

[59] S. Kim, A. Sin, H. Nam, Y. Park, H. Lee, C. Han, *Chem. Eng. J. Adv.* **2022**, *9*, 100213.

[60] A. Fazli, M. Brigante, A. Khataee, G. Mailhot, *Appl. Surf. Sci.* **2021**, *559*, 149906.

[61] Z. Yang, Y. Li, G. Zhang, *Chemosphere* **2024**, *357*, 141939.

[62] L. Dai, Z. Lei, Y. Cao, M. Zhang, X. Song, G. Wang, G. Ma, T. Zhao, J. Ren, *J. Environ. Chem. Eng.* **2024**, *12*, 112261.

[63] M. Adeel, V. Granata, G. Carapella, L. Rizzo, *J. Hazard. Mater.* **2024**, *465*, 133102.

[64] K. Bule Možar, M. Miloloža, V. Martinjak, F. Radovanović-Perić, A. Bafti, M. Ujević Bošnjak, M. Markić, T. Bolanča, M. Cvetnić, D. Kučić Grgić, Š. Ukić, *Water* **2024**, *16*, 673.

[65] Q. Chen, L. Wan, H. Zhou, F. Luo, L. Lei, N. Wang, *J. Water Process Eng.* **2023**, *56*, 104343.

[66] P. García-Muñoz, P. H. Allé, C. Bertoloni, A. Torres, M. U. de la Orden, J. M. Urreaga, M.-A. Dziurla, F. Fresno, D. Robert, N. Keller, *J. Environ. Chem. Eng.* **2022**, *10*, 108195.

[67] A. Fazli, S. Lauciello, R. Brescia, R. Carzino, A. Athanassiou, D. Fragouli, *Appl. Catal. B Environ. Energy* **2024**, *353*, 124056.

[68] G. Pulido-Reyes, L. Magherini, C. Bianco, R. Sethi, U. von Gunten, R. Kaegi, D. M. Mitrano, *J. Hazard. Mater.* **2022**, *436*, 129011.

[69] L. Tian, Q. Chen, W. Jiang, L. Wang, H. Xie, N. Kalogerakis, Y. Ma, R. Ji, *Environ. Sci. Nano* **2019**, *6*, 2907.

[70] C. di Luca, J. Garcia, D. Ortiz, M. Munoz, J. Carbajo, Z. M. de Pedro, J. A. Casas, *J. Environ. Chem. Eng.* **2023**, *11*, 110755.

[71] Y. Cai, F. Chen, L. Yang, L. Deng, Z. Shi, *Water* **2023**, *15*, 1920.

[72] C. A. Rojas-Guerrero, M. Villanueva-Rodríguez, J. L. Guzmán-Mar, A. Hernández-Ramírez, E. I. Cedillo-González, F. E. Longoria Rodríguez, L. Hinojosa-Reyes, *J. Environ. Chem. Eng.* **2023**, *11*, 110415.

[73] H. Luo, Y. Zeng, Y. Zhao, Y. Xiang, Y. Li, X. Pan, *J. Hazard. Mater.* **2021**, *413*, 125342.

[74] V. P. Kelkar, C. B. Rolsky, A. Pant, M. D. Green, S. Tongay, R. U. Halden, *Water Res.* **2019**, *163*, 114871.

[75] A. Khataee, A. Fazli, M. Fathinia, F. Vafaei, *Ozone Sci. Eng.* **2019**, *41*, 35.

[76] A. Khataee, A. Fazli, M. Fathinia, F. Vafaei, *J. Clean. Prod.* **2018**, *186*, 475.

[77] N. Ormeno-Cano, J. Radjenovic, *J. Hazard. Mater.* **2022**, *431*, 128462.

[78] L. Seid, D. Lakhdari, M. Berkani, O. Belgherbi, D. Chouder, Y. Vasseghian, N. Lakhdari, *J. Hazard. Mater.* **2022**, *423*, 126986.

[79] B. Jiang, J. Zheng, S. Qiu, M. Wu, Q. Zhang, Z. Yan, Q. Xue, *Chem. Eng. J.* **2014**, *236*, 348.

[80] J. Ren, J. Li, Y. Zhen, J. Wang, Z. Niu, *Sep. Purif. Technol.* **2022**, *290*, 120832.

[81] A. O. Adeola, B. A. Abiodun, D. O. Adenuga, P. N. Nomngongo, *J. Contam. Hydrol.* **2022**, *248*, 104019.

[82] M. Al-Sid-Cheikh, S. J. Rowland, K. Stevenson, C. Rouleau, T. B. Henry, R. C. Thompson, *Environ. Sci. Technol.* **2018**, *52*, 14480.

[83] W. Fu, J. Min, W. Jiang, Y. Li, W. Zhang, *Sci. Total Environ.* **2020**, *721*, 137561.

[84] L. Hildebrandt, D. M. Mitrano, T. Zimmermann, D. Pröfrock, *Front. Environ. Sci.* **2020**, *8*.

[85] K. B. Gavazov, I. Hagarová, R. Halko, V. Andruch, *J. Mol. Liq.* **2019**, *281*, 93.

[86] P. Wu, Y. Tang, G. Cao, J. Li, S. Wang, X. Chang, M. Dang, H. Jin, C. Zheng, Z. Cai, *Anal. Chem.* **2020**, *92*, 14346.

[87] D. Magrì, P. Sánchez-Moreno, G. Caputo, F. Gatto, M. Veronesi, G. Bardi, T. Catelani, D. Guarnieri, A. Athanassiou, P. P. Pompa, D. Fragouli, *ACS Nano* **2018**, *12*, 7690.

[88] F. Lionetto, C. E. Corcione, A. Rizzo, A. Maffezzoli, *Polymers* **2021**, *13*, 3745.

[89] A. Fazli, M. Brigante, A. Khataee, G. Mailhot, *Chemosphere* **2022**, *291*, 132920.

[90] D. Magrì, M. Veronesi, P. Sánchez-Moreno, V. Tolardo, T. Bandiera, P. P. Pompa, A. Athanassiou, D. Fragouli, *Environ. Pollut.* **2021**, *271*, 116262.

[91] D. Jia, Q. Li, K. Hanna, G. Mailhot, M. Brigante, *Environ. Pollut.* **2021**, *288*, 117728.

[92] L. D. B. Mandemaker, F. Meirer, *Angew. Chem. Int. Ed.* **n.d.**, *n/a*, DOI 10.1002/anie.202210494.

[93] X.-D. Sun, X.-Z. Yuan, Y. Jia, L.-J. Feng, F.-P. Zhu, S.-S. Dong, J. Liu, X. Kong, H. Tian, J.-L. Duan, Z. Ding, S.-G. Wang, B. Xing, *Nat. Nanotechnol.* **2020**, *15*, 755.

[94] Y.-S. Chang, S.-H. Chou, Y.-J. Jhang, T.-S. Wu, L.-X. Lin, Y.-L. Soo, I.-L. Hsiao, *Sci. Total Environ.* **2022**, *814*, 152675.

[95] T. Yang, J. Luo, B. Nowack, *Environ. Sci. Technol.* **2021**, *55*, 15873.

[96] X. X. Han, R. S. Rodriguez, C. L. Haynes, Y. Ozaki, B. Zhao, *Nat. Rev. Methods Primer* **2022**, *1*, 1.

[97] L. Xie, K. Gong, Y. Liu, L. Zhang, *Environ. Sci. Technol.* **2023**, *57*, 25.

[98] P. Li, Q. Li, Z. Hao, S. Yu, J. Liu, *J. Environ. Sci.* **2020**, *94*, 88.

[99] D. Materić, A. Kasper-Giebl, D. Kau, M. Anten, M. Greilinger, E. Ludewig, E. van Sebille, T. Röckmann, R. Holzinger, *Environ. Sci. Technol.* **2020**, *54*, 2353.

[100] J. Delgado-Gallardo, G. L. Sullivan, P. Esteban, Z. Wang, O. Arar, Z. Li, T. M. Watson, S. Sarp, *ACS EST Water* **2021**, *1*, 748.

[101] M. Meyns, F. Dietz, C.-S. Weinhold, H. Züge, S. Finckh, G. Gerdts, *Anal. Methods* **2023**, *15*, 606.

[102] L. Nigamatzyanova, R. Fakhrullin, *Environ. Pollut.* **2021**, *271*, 116337.

[103] W. Zhang, Q. Wang, H. Chen, *Front. Environ. Sci. Eng.* **2021**, *16*, 11.